IOSR Journal of Applied Chemistry (IOSR-JAC)
e-ISSN: 2278-5736.Volume 7, Issue 12 Ver. II. (Dec. 2014), PP 32-44
www.iosrjournals.org

Nanoindentation Behaviorand Physical Properties of Polyvinyl Chloride /Styrene co-maleic anhydride Blend Reinforced by Nano-Bentonite

D. E. Abulyazied[1*], S. M. Mokhtar[2], A. M. Motawie[1],
1Polymer Laboratory, Petrochemical Dept., Egyptian Petroleum Research Institute, Nasr City, Cairo, Egypt, Postal code: 11727
2Chemistry Dept., College of girls, Ain Shams University, Cairo, Egypt, Postal code: 11715

Abstract: *This article studiesthe effects of nano-bentonite on the structure and properties of polymer blends nanocomposites, based on polyvinyl chloride (PVC) and styrene co-maleic anhydride (SMA) blend. Modification of Egyptian bentonite (EB)is carried out using organo-modifier namely; octadecylamine (ODA). Octadecylamine bentonite (ODA-B) is characterized using FTIR, XRD and TEM. Nanocomposites of PVC/SMA/ODA-B are prepared by solution intercalation polymerization from 0.50 up to 5 phr. The nanocomposites are characterized by XRDand TEM. Thermalbehavior of the nanocomposites is studied.The effect of different content of ODA-B on the nano-mechanical properties is investigated by a nanoindentation test method.Also the swelling and electrical properties of the nanocomposites are measured. The morphology of the nanocomposites shows that ODA-B achieved good dispersion in the PVC/SMA matrix. The thermal stability of the nanocomposites is enhanced due to the presence of the ODA-B. Incorporation of 0.5, 1, 3 and 5 phr.ODA-B into the PVC/SMA blends results in an improvement in nano-hardness of 16%, 76%, 92%, and 68% respectively. The elastic modulus increased by 37% from 4.59 GPa for unreinforced PVC/SMA blend to 6.30 GPa for 3 phr. The cross-link density and the electrical conductivity of the nanocomposites areincreasedwith increasing the content of ODA-B.*

Keywords:*PVC, SMA, nanocomposites, nano-bentonite, nanoindentation, crosslink density.*

I. Introduction

Nanocomposites are considered as the next industrial revolution materials. What differentiates nanocomposite materials from classical composites is the degree of control in fabrication, processing and performance that can be achieved nearly down to the atomic scale. In the present age, the main focus area is in identifying a nanocomposite material which is lighter in weight, eco-friendly, bio-degradable, cost-effective, performance-oriented as well as suited for diverse applications. One way of achieving some of the above functionalities is by using organic and natural materials as filler material in different polymer blends.[1]

Polyvinyl chloride (PVC), as an important commercial polymer, has been studied and used widely in industrial fields for many years. Polyvinyl chloride exists as two distinctly different thermoplastics, rigid PVC and flexible PVC, which are used in a wide variety of applications. [2]However, due to its inherent disadvantages, such as low thermal stability and brittleness, PVC and its composites are subject to some limitations in certain applications.[3] Therefore, it is necessary to develop new PVC products with altered properties in order to broaden PVC applications, and this achieved by blending it with polymer to enhance its shortcoming.[4]Polymer blends represent an important class of materials in engineering applications. The incorporation of clay nano-filler may provide new opportunities for this type of materials to enhance their applications.

SMA polymers with a high molecular weight are widely used in engineering plastic applications, normally in the impact modified and optional glass fiber filled variants. Alternatively, SMA is applied using its transparency in combination with other transparent materials like PMMA or the heat resistance to heat-boost other polymer materials like ABS or PVC.[5]

Clay/ polymer nanocomposite materials have attracted great interest because nanoclays can reinforce almost all types of polymer matrices with similar properties than traditional composites, but less weight and better processability.[6]Various studies were conducted on PVC/clay nanocomposites under different curing conditions. The exfoliated clay structure possesses superior properties and gives a few advantages over other nano-fillers like in terms low cost and environmental friendly matters.[1]

Nanoindentation is a promising way of measuring the mechanical properties of materials at smaller length and load scales than allowed by other testing methods, thus allowing individual constituents to be examined. [5] Nano and micromechanical testing involves the use of rigid indenters, typically with diamond or diamond-coated tips. [6] Nanoindentation is also known as depth sensing indentation and involves obtaining

quantitative force versus displacement data and determining the elastic modulus, E, and nano-hardness values, H, of materials even beyond their elastic limit. Knowledge of such mechanical properties at the nano level can be important for certain material selection and design criteria and applications reinforcement on nano-mechanical properties.[7]

In this context, the aim of this work is to find out what type of changes will cause the nano-bentonite to be incorporated in the polymer blend of PVC and SMA, and how those changes will affect the thermal, mechanical, swelling and electrical properties of the resulting nanocomposite.

II. Experimental

2.1. Materials

All the materials under investigation are commercially available products. The general purpose polyvinyl chloride PVC resin used was a white powder made by suspension polymerization with k value of 70 and Tg 87°C. It was supplied by Petrochemical Industrial Co. (Alexandria, Egypt). Dioctyl phthalate (DOP), calcium stearate, tribasic lead sulphate and neutral lead stearate stabilizers were of technical grade and supplied by North China PlasticAssistant Factory (BaoDing, China).SMA was purchased from Polyscope, polymers (BV), Netherland, Code: XIRAN^R, MA: St 40:60 and average M.wt: 6094. Egyptian Bentonite EB, was supplied from south of El-Hamamm district, saving at 0.6 micron. It was dried at 80 °C for 24 h under vacuum conditions. (Reported basal plane spacing, d001 = 1:26 nm).Octadecyle amine (ODA) CH_3 $(CH_2)_{17}NH_2$, (Mw 269.51 gm/mole), hydrochloric acid and sodium chloride, tetrahydrofurane THF, were provided by Aldrich, USA.

2.2. Preparation of Organo–Bentonite

Egyptian Bentonite EB was purified to remove impurities, i.e. carbonates, iron hydroxide and organic matter, and then activated to Na bentonite (Na-B) according to amethod mentioned in a previous work. [8, 9] The organo-bentonite was synthesized by ion exchange reaction between Na-B and ODA using equation (1).

$$\frac{120}{100} * \text{ grams of clay} * 1.5 = \frac{X}{M_w \text{ of intercalting agent}} * 1 * 1000 \quad \ldots\ldots\ldots\ldots\ldots (1)$$

Where; X represents the amount of intercalating agent used, 120/100 represents the cationic exchange capacity CEC of 120 meq/100 g of the bentonite(the CEC is determined in our patent, [8] and 1.5 (> 1) is the alkyl amine/bentonite ratio, whichindicates an excess amount of intercalating agent being used. The molar alkyl amine/HCl ratio was 1:1. The method of modification is explained in details in the previous work.[8, 9]

2.3. Preparation of PVC/SMA/ODA nanocomposites:

The solution of PVC resin (50 phr) and SMA (50 phr) in THF prepared in two separately a dark laboratorybottles, by slowly mixing during 24 h at an ambient temperature. The two polymer solutions were then mixed together. Thereafter, PVC/SMA solution was mixed withvarious ODA-B contents (0, 0.50, 1, 3 and 5phr) usingsonicator, VCX-750 (Sonics and materials, Inc.) equipped with a titanium Probe (diameter 13 mm) withfrequency of 20 KHz for, 5-15 min at room temperature, toachieve the distribution of ODA-B in the blend matrix ashomogeneous as possible. Calcium stearate (0.2phr), tribasic lead sulphate (6phr), neutral leadstearate (0.2phr) as heat stabilizer, and DOP (50phr) as plasticizer were added to all formulationsas listed in Table 1. The cast films from the PVC/SMA blank sample and PVC/SMA/ODA-B nanocomposites were prepared on a glass surface, and thendried in vacuum. [10]

Table 1: Formulations of PVC/SMA/ODAnanocomposites

Ingredients	Content (phr.)
PVC	50
SMA	50
DOP	50
Calcium stearate	0.2
Tribasic lead sulfate	0.6
Neutral lead stearate	0.2
ODA-B	0, 0.5, 1, 3, 5

2.4. Characterizations

2.4.1. Fourier-Transform Infrared Analysis (FTIR)

The surface chemistry of the powdered fillers was characterized by Fourier-Transform Infrared Analysis (FTIR) operated in the transmission mode, in the wave number range of 4000- 400 cm^{-1}, by mixing with KBr powder on a Mattson 1000, series LC operating, Issue I (0791) spectrophotometer. The concentration

of the samples in the KBr was held constant to 0.7% (w/w). The spectra were obtained using a resolution of 4 cm^{-1} and were averaged over 100 scans. Standard software (Omnic ESP, version 5.1) was used for data acquisition and analysis.

2.4.2. X-ray Diffraction Analysis XRD

X-ray diffraction (XRD) measurements were performed on X'Pert Pro diffractometer manufactured by Panalytical with Cu Kα radiation (λ= 0.154 nm, 45 KV and 30 mA) at room temperature (25 °C).

2.4.3. Transmission Electron Microscopy (TEM)

High resolution transmission electron microscopy (HRTEM) was adopted to characterize the nano-particles modification. TEM was performed by TEM-1230 with an accelerating voltage of 200 KV (JEOL Co., Japan). The nanoparticles were sectioned into ultra-thin slices (100 nm) at room temperature using a microtome and then mounted on 200 mesh copper grids.

2.5. Measurements for nanocomposites:

2.5.1. Thermal Properties

The thermal stability was determined by thermogravimetric analysis (TGA) witha Shimadzu TGA-50H using 8-10 mg sample. The sample was heated at a rate of 10° C/min in the range 50 - 600 ° C in nitrogen atmosphere.

2. 5.2. Nanoindentation Testing

Low load nanoindentation tests in this study were performed by Nano Test Vantage apparatus, (Micro Materials Co, UK, 2012). A spherical diamond indenter tip manufactured by Micro Materials was used. The specimens were mounted onto the nano-indentation fixture using a suitable adhesive. All tests were conducted at an approximate temperature of 27 °C. Typical experimental indentation parameters used for all measurements were as follows:

Minmum load: 10 mN, the maximum load for all indents: 50 mN, Dwell time or holding time at maximum load: 20 s and number of indentation: 25 indent.

2.5.3. Swelling Properties

All samples of known weight (m_o) were immersed in thimbles containing solvents with different cohesive energy densities ( ), as presented in Table 2.The swelling measurements were carried out at 25°C for various time intervals. The samples were then removed, blotted quickly to remove the attached solvent on the sample surface and weighed. The swelling equilibrium was reached after 24 h. The degree of swelling has been calculated using the relation:

$$Q\% = \frac{m - m_o}{m_o} * 100 \quad \text{……...…...……} \ (2)$$

wherem_o and m are the masses of the sample before and after swelling.

For all samples, swelling data were used to calculate the volume fraction, V_m, and equilibrium degree of swelling, Q_m, of the polymers in a given sample swollen to equilibrium in solvent. [11]

$$Q_m = (1 + \frac{\rho (Q_w - 1)}{d}) \quad \text{.....(3)}$$

where Q_w is the ratio of the weights of the network in the swollen and dry state, while ρand d are the densities of the sample and solvent, respectively. The equilibrium degree of swelling, Q_m, was defined as $Q_m = 1/ V_m$.

Table 2: The molar volume V_1, solubility parameters (δ), and densities (d)of the solvents used

Solvent	V_1 (cm^3 mol^{-1})	δ (J cm^{-3})$^{0.5}$	Density (g cm^{-3})
Water	18	47.84	1
Methanol	40.6	29.65	0.79
Ethanol	58.3	25.96	0.79
Butyl alcohol	91.4	23.31	0.92
Acetone	73.5	20.24	0.79
Methyl ethyl ketone	90.1	19.01	0.805
Benzene	88.7	18.81	0.88
Toluene	105.9	18.22	0.87
xylene	124	18.09	0.86
Carbon tetrachloride	96.9	17.68	1.5867
cyclohexane	109.2	16.58	0.779
Kerosene	180	15.64	0.78–0.81
Hexane	132.4	14.80	0.6548

2.5.4. Electrical Properties

The electrical measurements were carried out using a DC voltage/ current generator, along with a precision digital electrometer (Keithley 6517A) to determine the current generated on application of a known voltage to filled polymer. The measurements were made at different temperatures for all samples.

III. Results and Discussion

3.1. Characterization of nano-bentonite:

3.1.1.FTIR Analysis:

The structure of the prepared nano–bentonite ODA-B is confirmed by FTIR spectra measurement. The FTIR spectra of the unmodified Na-B and the nano-bentonite ODA-B is shown in Fig. 1.

FTIR spectrum of Na-B in figure (1) indicates that the OH bending band at 915 cm^{-1} was readily assigned to Al-OH. The strong band centered at 1029 cm^{-1} (Si-O stretching vibrations) together with those at 524 cm^{-1} and 463 cm^{-1} (Si-O-Al and Si-O-Si bending vibration, respectively) were typical of tetrahedral Si-O. Bands at 3426 and 1637 cm^{-1} were attributed to the OH stretching and bending vibrations of molecular water, respectively. [12, 13] Band at 1475 cm^{-1} was assigned to the presence of carbonate. [14]

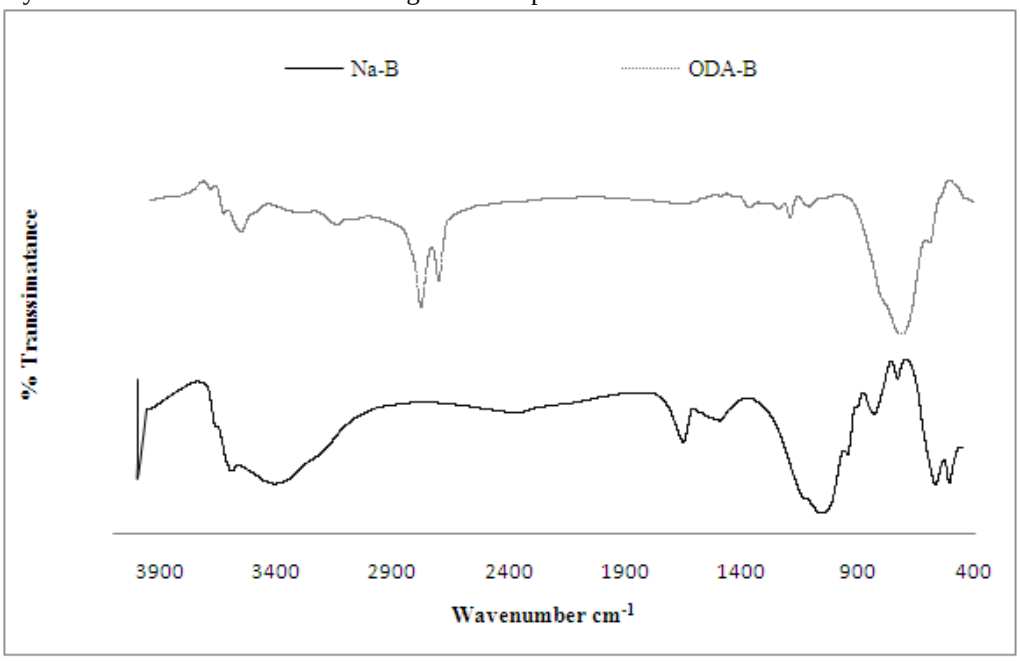

Fig. 1: FTIR Spectrum of (a) unmodified Na- B and the modified ODA-B.

The spectra of ODA-B give all the previous bands which appeared in the FTIR spectrum of Na-B in(Fig. 1). These bands are related to the basic skeleton of the bentonite, but there are new features in (Fig. 1) that are related to the intercalated organo- modifier. Peaks at 2915 and 2840 cm^{-1} were assigned to the stretching vibration of $–CH_2$ and $–CH_3$, respectively, indicating the presence of long alkyl chain in the bentonite. Bands at 3426 and 1637 cm^{-1} which were attributed to the OH molecular water disappeared. This indicates complete exchange of basal cations with the removal of water molecules. [15]

3.1.2. X-Ray diffraction

The structures and the variations of the silicate-gallery spacing (d_{001}) of the unmodified Na-B and the modified ODA-B were detected by wide angle X-ray diffraction (Fig.2.).

It is clear from the pattern that, from 2θ =2 to 10˚, the Na-B has a single characteristic diffraction peak at (2θ) = 7.0˚ indicating that the d-spacing of the silicate layers was about 1.2 nm. [16] A shift of the d-spacing of the modified bentonites to lower diffraction angles by comparison to the unmodified Na-B, is shown in (Fig.2). These results reveal that the layer gallery of bentonite expanded due to the modification of the surfactant, which contained a long-chain alkyl group.

Fig.2. also shows that, ODA-B gives two characteristic peaks at two different 2θ. The higher extent of intercalation corresponds to the large interlayer distance of 3.09 nm at 2θ =2.9˚ as compared with 1.26 nm for Na-B. This value of d-spacing indicates that ODA gives high separation for the clay layers. [8, 9]The other characteristic peak of ODA-B at 2θ=5.7˚ corresponds to basal spacing of 1.55 nm. The changes of interlayer spacing suggest the successful modification of Na-B. [17]

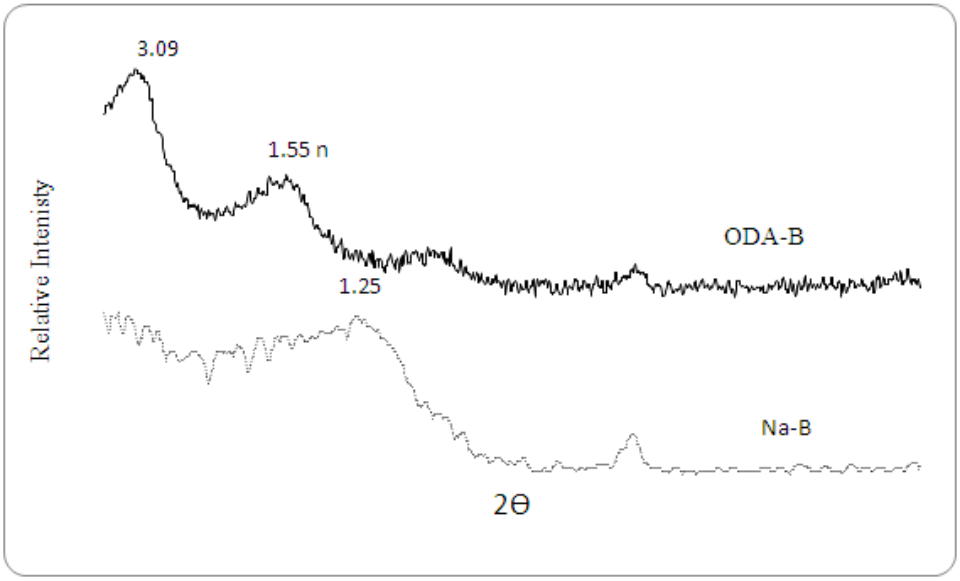

Fig.2. XRD pattern of Pristine Na-B and ODA-B

3.1.3. Transmission Electron Microscope TEM

Morphological study has been carried out in order to monitor the formation of the nano-particles. The TEM morphology of pristine unmodified bentonite is presented in (Fig. 3-a). It is clearly seen from this figure that the particles of the unmodified bentonite are in the agglomerated forms. The TEM photograph of the prepared ODA-B nanoparticles is shown in (Fig. 3-b) showing that the silicate layers are separated to some thin lamellas with a 10 nm thick. Also the images show ODA-B gives best dispersion.

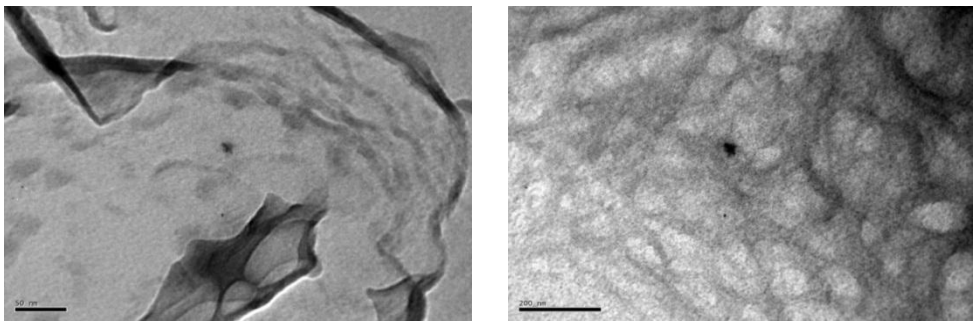

(a) (b)

Fig.3. TEM photographs of the EB: (a) unmodified Na-B as received and (b) ODA-B modified bentonite.

3.2. Characterization of PVC/SMA/ODA-B nanocomposites:

3.2.1. XRD of the nanocomposites

The XRD patterns of PVC/SMA/ODA-B nanocomposites at different content of the ODA-B are shown in (Fig.4). As seen from the Figure, the diffraction peak of ODA-B is almost invisible in the patterns for all the samples. This result suggests that the layered silicate galleries of the nanocomposites have been exfoliated in the PVC/SMA matrix, which will be confirmed by TEM.[18, 19]

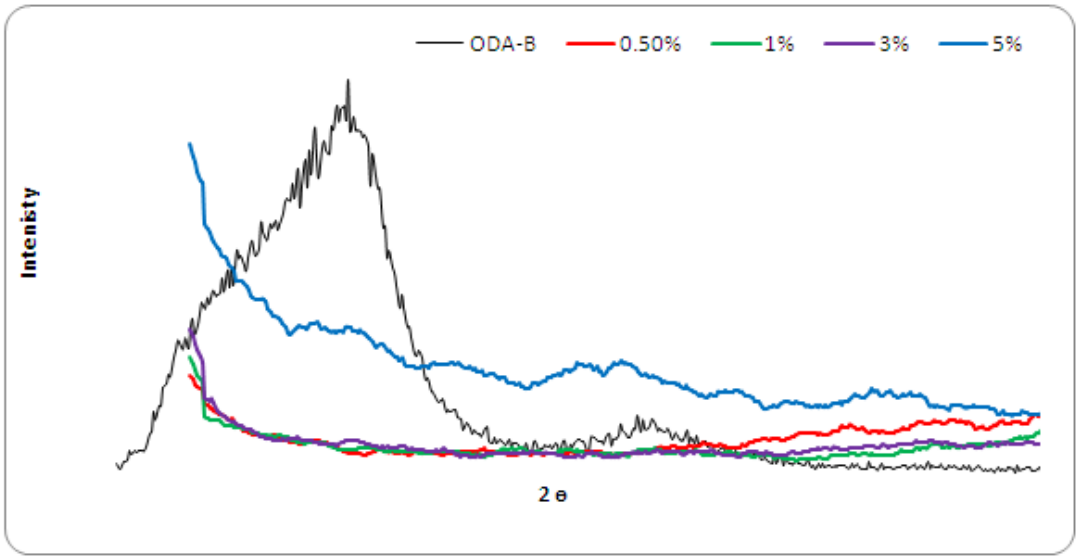

Fig.4: XRD pattern of PVC/SMA/ODA-B nanocomposites with different ODA-B content.

3.2.2. Transmission Electron Microscope TEM

The TEM micrographs of PVC/SMA/ODA-B nanocomposites are shown in Fig. 5. When using nano-clay particles as filler, because the nanoparticles have a strong tendency to agglomerate, their homogeneous dispersion in PVC/SMA is a difficult job. (Fig. 5-a,b and c) reveals the nanoscale dispersion of nano-bentonite in PVC/SMA matrix at 0.5, 1, and 3phr. From this figure, one could find that most of the nano-bentonites were dispersed as primary particles, while some nano-bentonites aggregated. It can also be observed that nano-bentonite is well dispersed in the PVC/SMA matrix in 3 phr. sample. More aggregates are found when the content of nano-bentonite is increased to 5phr., as shown in (Fig. 5-d). This is reasonable, considering that at high ODA-B content, the interparticle distance is small, and hence, agglomeration of these nanoparticles can occur during mixing and not all clay layers were separated from the clay tactoids. [20]

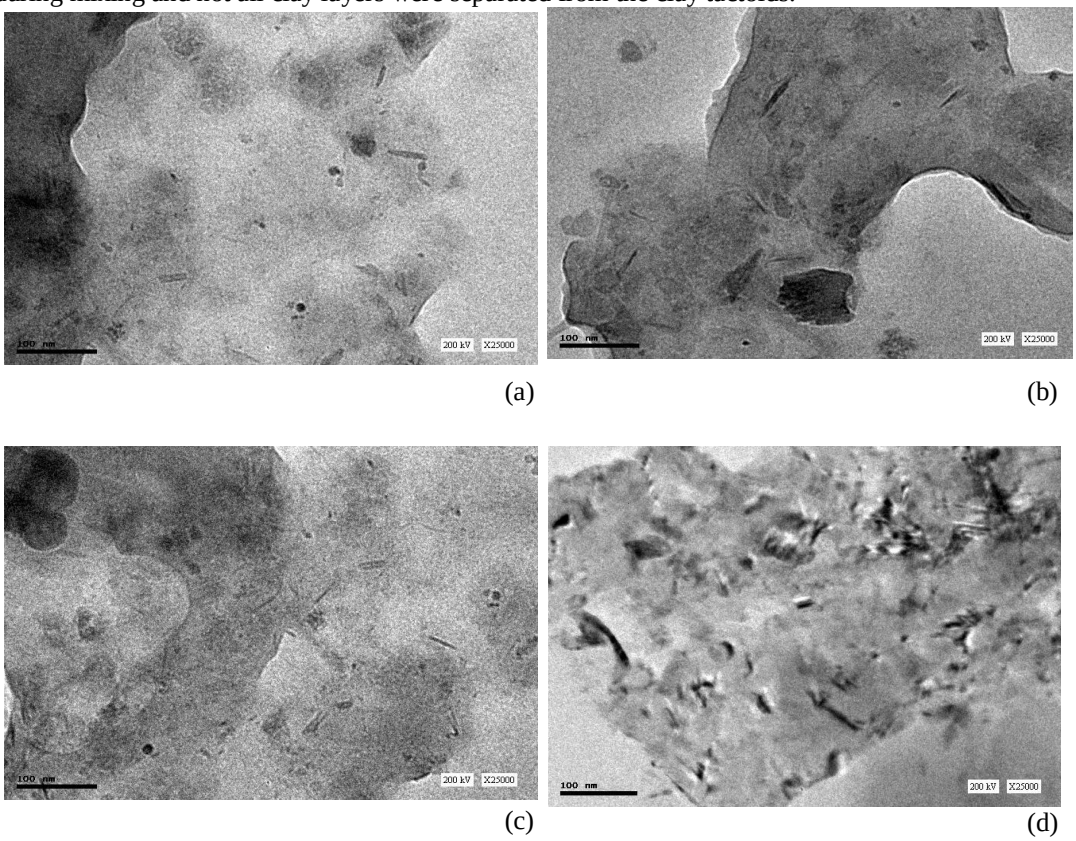

Fig.5. HRTEM images of PVC/SMA/ODA-B nanocomposites: (a) 0.5, (b) 1 (c) 3 and (d) 5 phr.

3.3 Effect of nano- bentonit on the physical properties of PVC/SMA blend

3.3.1. Thermal Properties

The thermal stability of polymeric blend is usually studied by thermo-gravimetric analysis (TGA). The weight loss due to the formation of volatile products after degradation at high temperature is monitored as a function of temperature. When heating occurs under an inert gas flow, a non-oxidative degradation occurs, while the use of air or oxygen allows oxidative degradation of the samples. Generally, the incorporation of clay into the polymer matrix was found to enhance thermal stability. [21]However, thermal behavior of polymer/clay nanocomposites is complicated and many factors contribute to the increase in thermal resistance. Due to thecharacteristic structure of the layers inthepolymer matrix and nanoscopic dimensions of filler particles, several effects have been observed that can explain the changes in thermal properties.

The TGA thermograms of the PVC/SMA/ODA-B nanocomposites and the unreinforced sample of blend are shown in (Fig.6). It is clearly seen from the curves that the starting decomposition temperatures of the nanocomposites were nearly equivalent to that of pure PVC/SMA blend. The decomposition temperatures of all samples at 5% and 50% loss of the weight were showed in Table 3.We could see from Table 3, the decomposition temperatures of 0.5, 1, 3 and 5 phr. at 5wt.% loss increased by 32, 9 12 and 6 °C respectively compared with unreinforced PVC/SMA blend. Also, thedecomposition temperatures at 50wt. % loss increased by 14, 21, 6 and 11 °C respectively, whichindicated that the thermal stability of the nanocomposites was enhanced.

The reason was perhaps that the nano-bentonite could easily disperse in the polymer matrix. [22]When the temperature was high enough to break up the chain of the polymers; the nano-bentonite could absorb the heat or limit the heat transfer due to the higher thermal stability of nano-bentonite. Meanwhile, the nano-bentonite could absorb small molecules released from the nanocomposites, prevent their escaping from the nanocomposites and further decelerate the decomposition of the polymers. [23, 24, and 25]At last, the char yield at 500 ◦C for nanocomposite series are higher than that of the blank sample. All these results confirm that the thermal stability of the PVC/SMA/ODA-B nanocomposites was enhanced due to the presence of the nano-bentonite.

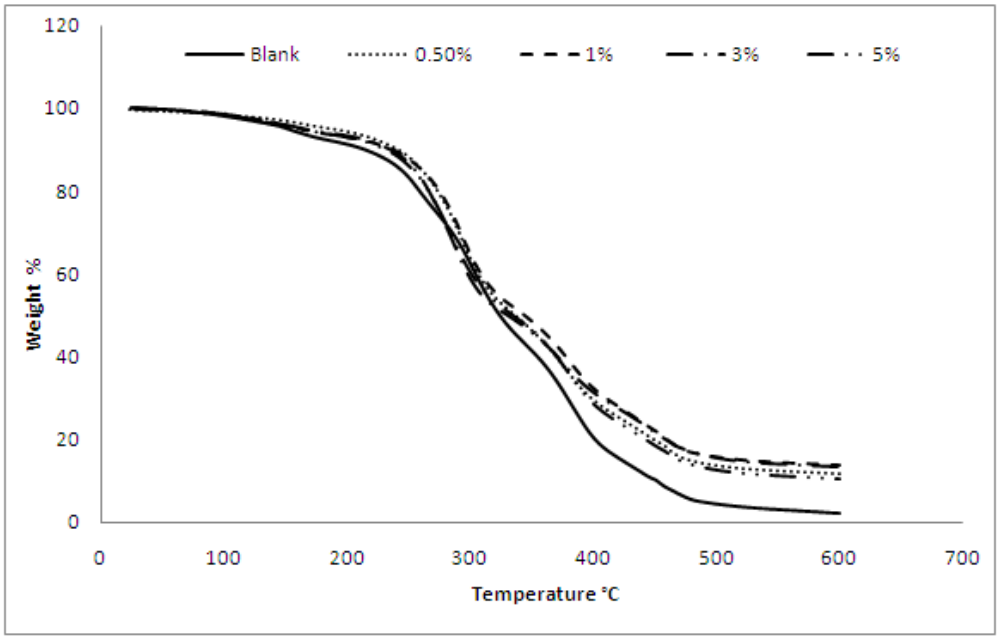

Fig.6: TGA curves of unreinforced sample and the nanocomposites with different ODA-B content.

Table (3): Thermal Parameters of the nanocomposites

ODA%	$T_{5\%}$ ºC	$T_{50\%}$ºC	char residue (wt%at 500 ºC)
Blank	139	319	0.378
0.50	171	333	0.428
1.00	148	340	0.417
3.00	151	325	0.551
5.00	145	330	0.482

3.3.2. Nanoindentation behavior

- **Maximum depth:**

The important quantities of the loading–unloading cycle are maximum load (P_{max}), maximum depth (h_{max}), final depth after unloading (h_f) and the slope of the upper portion of the unloading curve (S) known as the elastic contact stiffness. [7] A typical loading–unloading cycle data for an unreinforced blend and the nanocomposites samples is presented in (Fig.7). The average maximum depth at peak load for unreinforced sample is approximately 21864 nm, while for the nanocomposites are 19039, 13820, 12154 and 13820 for 0.5, 1, 3 and 5 phr. ODA-B reinforced samples, respectively. These values show that the depth at peak load for these samples is approximately about 14, 58, 74 and 58 % lower than that of the unreinforced blend sample.The extent of nano-bentonite dispersion may have contributed to higher resistance to plastic deformation leading to a lower indentation depth. [6]

Close observation of the load–unload curves (nano test indentations for unreinforced blend) indicates a uniform surface by virtue of the reproducibility of the 25 indents at different locations. Similarly, for 0.5,1, 3 and 5 phr. ODA-B loaded samples, in all experiments; both loading and unloading curves appear to be continuous and consistent. [26]

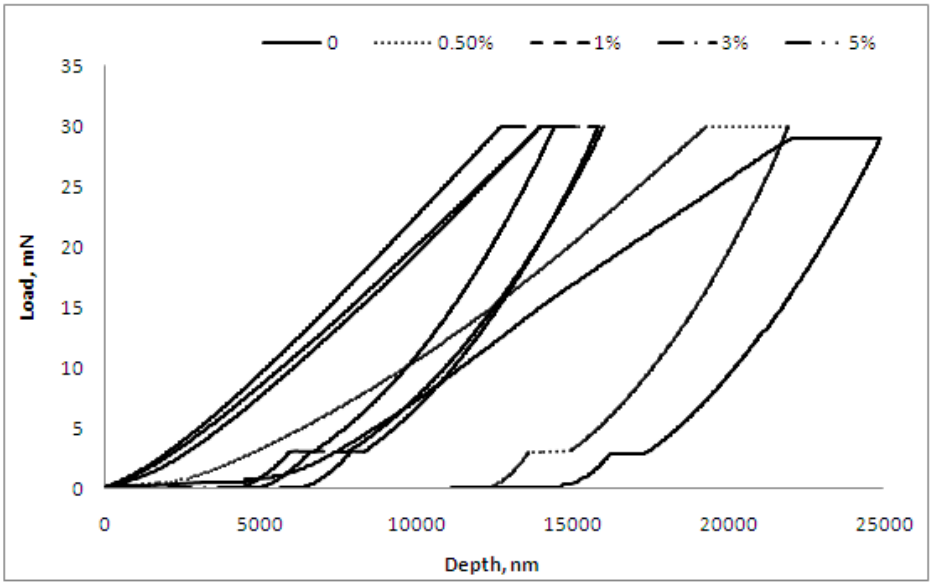

Fig.7: Typical loading hold unloading curves for unreinforced PVC/SMA and the nanocomposites.

- **hardness and elastic modulus**

The hardness and elastic modulus can be derived using the method developed by Oliver and Pharr. [27]The fundamental relationships to calculate the hardness, H and modulus, E are:

$$H = \frac{P_{max}}{A} \dots\dots\dots\dots\dots\dots\dots\dots\dots\dots (4)$$

Where P_{max} is the peak indentation load and A is the projected contact area at maximum load, and

$$E_r = \frac{\sqrt{\pi}}{2}\frac{dP}{dh}\frac{1}{\sqrt{A}} \dots\dots\dots\dots\dots\dots\dots\dots\dots\dots (5)$$

Where, E_r is the reduced elastic modulus which accounts for the fact that elastic displacement occurs in both indenter and sample, and dP/dh = S. The elastic modulus of the test material, E_s, is calculated from E_r, the reduced modulus, obtained from the test using:

$$\frac{1}{E_r} = \frac{(1-\nu_s)^2}{E_s} + \frac{(1-\nu_i)^2}{E_i} \dots\dots\dots\dots\dots\dots\dots\dots\dots\dots (6)$$

where, $\nu_s$is the Poisson's ratio for the sample; (for polymer approximately 0.2), ν_i the Poisson's ratio for the indenter (for diamond 0.07), E_s the elastic modulus for the sample and E_i the elastic modulus for the indenter (1141 GPa is often used for a diamond). By rearranging Eq. (6), the equation for elastic modulus of the sample E_s is:

$$E_s = \frac{1-(\nu_s)^2}{\frac{1}{E_r} - \frac{1-(\nu_{si})^2}{E_i}} \dots\dots\dots\dots\dots\dots\dots\dots\dots\dots (7)$$

The nano-hardness and elastic modulus values of the samples are given in Table (4).From the results shown in Table (4), it can be seen that nano-betonite has a clear reinforcement effect on the PVC/SMA blend,whereby the hardness and modulus of all the nanocomposite samples are significantly higher than the un-reinforced PVC/SMA blend sample. [28] Compared with the neat PVC/SMA blend sample, nano-hardness increased by 16, 76, 92 and 68 % from (0.25 to 0.29, 0.44, 0.48 and 0.42 GPa) and the eleastic modulus increased by 13, 21, 37 and 28 % (from 4.59 to 5.21, 5.57, 6.30 and 5.88 GPa) for the nanocomposites containing 0.5, 1, 3 and 5 phr. ODA-B respectively. The mechanisms of improvement in the nano-hardness and the elastic modulus for the PVC/SMA blend matrix can be explained as the positive effect of high aspect ratio of nano-bentonite reinforcement. It is possible to say that the intermolecular interaction of nan-bentonite into PVC/SMA blend was improved up to 5 phr. as evidenced from the morphology study. [29]

Table (4): Summary of nanoindentation test results

ODA-B,phr.	Hardness, Gpa	Elastic modulus, Gpa
0	0.25	4.59
0.5	0.29	5.21
1	0.44	5.57
3	0.48	6.30
5	0.42	5.88

3.3.3.Swelling measurements

The maximum degree of swelling Q_m% in water for PVC/SMA/ODA-B nanocomposites as a function of ODA-B loading is shown (Fig.8). Q_m% decreases with the addition of ODA-B to PVC/SMA and is lowest for 3 phr., The platelet structure of nano-bentonite and its high aspect ratio enhanced the polymer/nano-bentonite interaction, hence leading to the decrease in free volume and consequently increase the degree of cross- linking. It is also ascribed to the comparatively homogeneous distribution of nano-bentonites in the polymer chain resulting in the compact packing between the polymer chains and the nano-bentonite which reduces the solvent uptake of PVC/SMA matrix during swelling. The influence of filler content on the properties of reinforced composites has been extensively reported in the literature. [30]It is generally agreed that the decrease in Q_m% is due to the strong interactions between polymer chains and ODA-B particles, and/ or between clayparticles itself. [31, 32]At high filler content at5 phr., the increase in Q_m% could be explained in terms of the aggregation of filler particles and poor polymer/filler interaction at higher concentration of nano-bentonite which could increase solvent uptake. [33, 34 and 35]

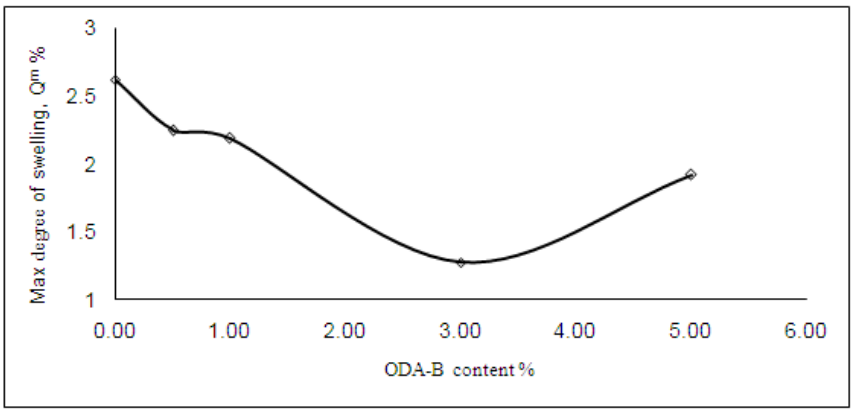

Fig. 8: Variation of maximum degree of swelling with ODA-B content for nanocomposites.

3.3.4. Determination the cross- linking density

Physical nature of crosslinked materials can be further characterized by calculation of their volume average network density. Several models have been developed to relate a measured quantity to practical molecular information, [36, 37] such as entanglement molecular weight, molecular weight between crosslinks. The most traditional methods are equilibrium swelling and mechanical measurements. The number of crosslinks in a unit volume is called crosslink density and is correlated with the molecular weight of the chain between two crosslink junctions (Mc) by [36, 38]:

$$\nu_e = \frac{\rho_p N}{\bar{M}_c} \quad \text{.....(8)}$$

where ρ_p is the polymer density, N is Avogadro's number.

Several theories have been proposed to calculate the molecular weight between cross- links in a polymer. Probably the most widely used of these theories is that of Flory and Rehner. [39]According to the theory of Flory and Rehner, for a perfect network;

$$\bar{M}_c = -V_1 \rho_p \frac{(V_m^{1/3} - V_m^{1/2})}{\ln(1-V_m) + V_m + \chi_1 V_m^2} \quad \ldots\ldots\ldots\ldots\ldots\ldots\ldots\ldots\ldots (9)$$

where $V_1$is the molar volume of the solvent, $V_m$is the volume fraction, and χ_1 is the Flory- Huggins interaction parameter between solvent and polymer.χ_1 can be calculatedwith the solubility parameter (δ), which is related to the cohesive energy density (CED) induced by van der Waals interactions. A physical quantity, termed the cohesive energy density, can be a useful parameter to help explain, quantify, or even predict the behavior in terms of barrier properties of polymeric materials. χ_1 may be expressed as follows [34,40]:

$$\chi_1 = \frac{(\delta_1 - \delta_2)^2 V_1}{RT} \quad \ldots\ldots\ldots\ldots\ldots\ldots\ldots\ldots(9)$$

where δ_1 and $\delta_2$are the solubility parameters or (CEDs) forthe solvent and polymer, respectively, and R is the universal gas constant. [40]The solubility parameter of the PVC/SMA blend was determined by plotting the degree of swelling at equilibrium of the sample in different solvents (with different CED, Table (2)) against the CED of the solvents (Fig. 9). The maximum at the abscissa of the plot is corresponding to the CED of the PVC/SMA blend,which was found to be around 16.5 $(Jcm^{-3})^{1/2}$.

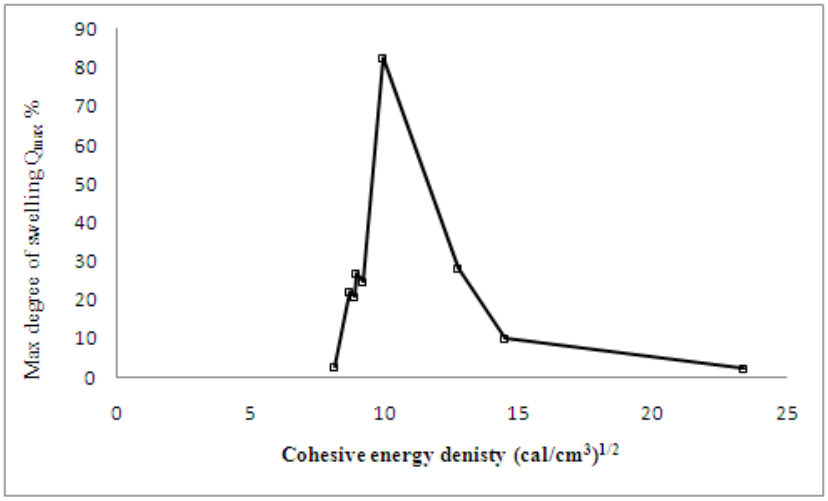

Fig. 9: The equilibrium swelling versus CED of liquids for PVC/SMA blank sample.

The calculated average cross-link density for all investigated samples at different filler loading is presented in (Fig.10) as a function of filler loading. The cross-link density values can be explained on the basis of Q_m%, which gives inverse behavior with filler loading.

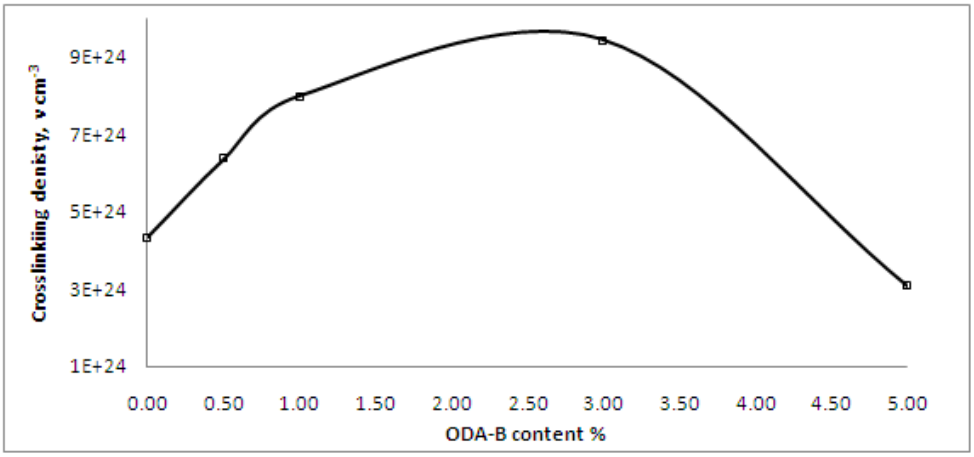

Fig.10: The average degree of cross-linking versus nano-bentonite loading for all the nanocomposites

3.2.4.Temperature Dependence of dc Conductivity:

(Fig.10) shows the variation of d.c. electrical conductivity with temperature for the PVC/SMA/ODA-B nanocomposites and the blank one over the temperature range 289 to 403 K. In general, the electrical conductivity is slightly thermally activated according to the well-known Arrhenius law in a way typical of semiconductors[41]:

$$\sigma = \sigma_o \exp(\frac{-E_a}{KT}).....(11)$$

σ_o is pre-exponential factor and inversely proportional to the temperature T, K is Boltzmann constant = $1.38x10^{-23}$ $J.K^{-1}$ andE_a is the activation energy.

It can be seen that the temperature dependence (Fig.11) has mainly two regions at low and high temperatures respectively, namely region I (289-333K) in which the conductivity is gradually increased with the increase in temperature, and region II (>333K) in which the change in, σ, is increased faster. The activation energy, E_a,for electrical conductivity of the two regions was determined and listed in Table (5).

The activation energy (E_a) value for PVC/SMA/ODA-B nanocomposites is less than that of the neat blend, as well as it drops with the increase in the ODA-B content in the composites, indicating that the process of conduction becomes easier. The final look at the table shows that the second activation energy region, E_2, is almost higher than that of the first region, E_1. This is due to the higher dissociation energy needed to form the charge carriers for the intrinsic conduction. [42, 43]

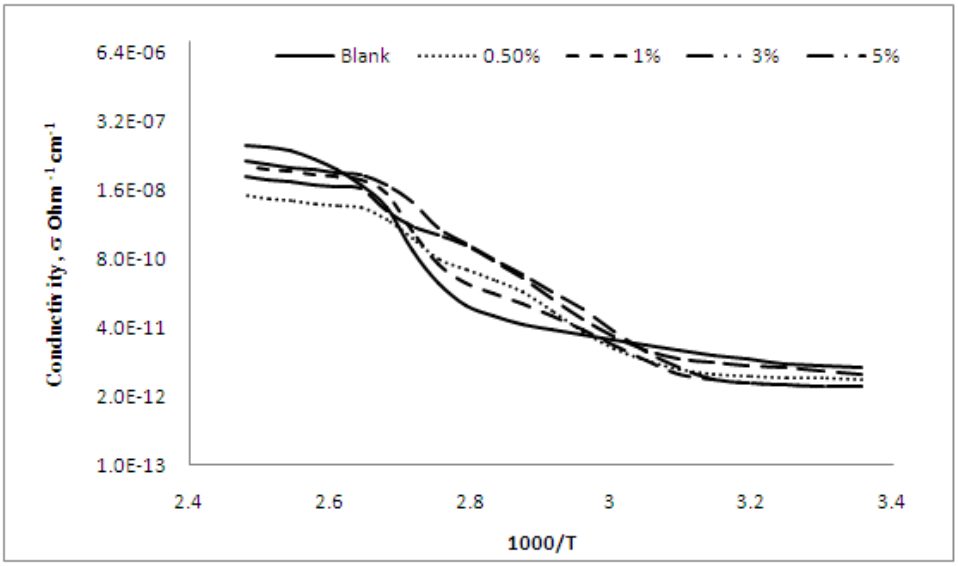

Fig.11: Temperaure dependence of dc. conductivity of PVC/SMA/ODA-B nanocomposites with different content of the ODA-B

Table (4): The activation energy of the dc conductivity in low (E_1) and high (E_2) temperature regions respectively at the different ODA-B content.

ODA %	ΔE_1 (ev)	ΔE_2 (ev)
0	0.05	1.11
0.5	0.03	0.71
1	0.05	0.80
3	0.01	0.78
5	0.07	0.74

Fig.12. shows the variation of the dc conductivity values at 80 °C for the PVC/SMA/ODA-B nanocomposites versus the weight percent of ODA-B in the nanocomposites. The Figure elucidates that the nano-bentonite is effective in producing nanocomposites with an increase in conductivity with the increase of ODA-B content. [39, 43]

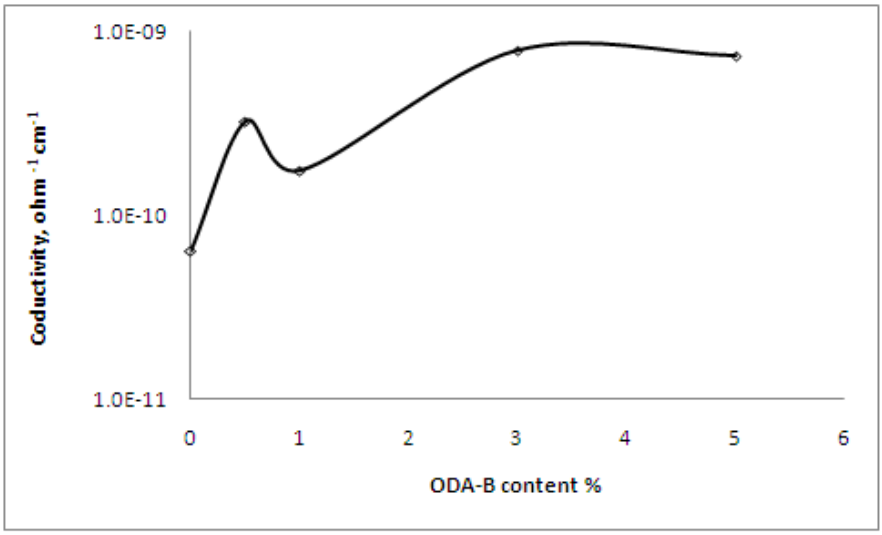

Fig.12: The dependence of the dc conductivities on the ODA-B loadings in the nanocomposite at 80 °C.

IV. Conclusion

Modification of the Egyptian Bentonite (EB) was carried out using organo-modifier namely; octadecylamine (ODA). The physical properties (thermal, mechanical, swelling and electrical) of the PVC/SMA/ODA-B nanocomposites were studied in details for different phr. of ODA-B. The preparation and characterization of PVC/SMA/ODA-B nanocomposites were also described in this study. The morphologywas characterized by XRD and TEM, and reveals good intercalation and exfoliation of nano-bentonite into the blend matrix. As a result, the PVC/SMA/ODA-B nanocomposites samples showed enhancement of their thermal stability, nano-hardness and modulus compared with the un-reinforced blend sample. The nano-hardness properties for nanocomposites specimens correspondingly increase with increasing ODA-B content. It can be concluded that the strengthening efficiency of nanocomposites increases with the content increase up to 5 phr. reinforcement. Also, the cross-link density values showedanincrease with the filler loading while inverse behavior was obtained for the maximum degree of swelling Q_m%. The temperature dependence of the dc conductivity has mainly two regions at low and high temperatures respectively. The activation energy, E_a, for electrical conductivity of PVC/SMA/ODA-B nanocomposites is less than that of neat blend, as well as it drops with the increase of the ODA-B content in blend matrix.Sample (3 phr.) of the nanocomposites gave the best data for all the properties of the nanocomposites which confirm the result of the TEM and confirm that it gave the best compact packing structure.

References

[1]. K.V.P. Chakradhar, K.V. Subbaiah, M.A. Kumar, G.R. Reddy'Epoxy/polyester blend nanocomposites: Effect of nanoclay on mechanical, thermal and morphological properties,Malaysian Polymer Journal, 6,2011, 109-118.
[2]. A.M.Motawie,A.A. Khalil, A.I.A. Eid, K.M. El-Ashry, E.M. Sadek, Some Studies on Poly (vinyl chloride)/Layered Silicate Nanocomposites Part 1, Morphology, Physico-mechanical, and Thermal Properties, Journal of Applied Science. Research, 9(10), 2013, 6355-6364.
[3]. Gilbert, M. Poly (vinyl chloride) (PVC)-based nanocomposites (Loughborough University, 2012).
[4]. S.A. Savrik, B.C. Erdogan, D. Balkose, S. Ulku, Statistical thermal stability of PVC, Journal of Applied Polymer. Science, 116,2010, 1811–1822.
[5]. L.G. Bourland, A.D. Wambach, PVC/styrene copolymer alloys for a balance of properties, Journal of Vinyl Technology, 5,1983, 121–125.
[6]. H.N. Dhakal, Z.Y. Zhang,M.O.W. Richardson, Nanoindentation behaviour of layered silicate reinforced unsaturated polyester nanocomposites, PolymerTesting, 25, 2006, 846-852.
[7]. G. Allegra, G. Raos,M. Vacatello, Theories and simulations of polymer-based nanocomposites: from chain statistics to reinforcement, Progress in Polymer Science, 33 (7),2008, 683-731.
[8]. Motawie, A. M.; Badr, M.M.;Abulyazied, D.E.;El-Komy, D.A. Egyptian Patent, 26250, 2013.
[9]. A.M. Motawie, M.M. Madany, A.Z. El-Dakrory, H.M. Osman, E.A. Ismail, M.M. Badr, D.A. El-Komy, D.E.,Abulyazied, Physico-Chemical Characteristics of Nano-Organo Bentonite Prepared Using Different Organo-Modifiers,Egyptian Journal of Petroleum,23 (3) 2014, In Press.
[10]. J. Shaojin, J. Pingkai, Z. Zhicheng, W. Zhongguang, Effect of carbon-black treatment by radiation emulsion polymerization on temperature dependence of resistivity of carbon-black-filled polymer blends, RadiationPhysics Chemistry, 75(4), 2006, 524-531.
[11]. N. A. Mansour, E. M. Sadek, G. M. Elkomy, S. I. Shara,A.M. Motawie,Some Studies on Poly (vinyl chloride) /carbon Nanocomposites,International Journalof Pure & Applied Chemistry, 6 (4),2011, ,409-414
[12]. R. Zagorka, M. Aleksandra, Study of montmorillonite and cationic activators sistem rheological characteristic change mechanism, Journal of European Ceramic society, 27 (2/3), 2007, 1691-1695.
[13]. C. Fenandes, C. Catrinescu,P. Castilho, Catalytic conversion of limonene over acid activated Serra de Dentro (SD) bentonite, Applied Catalyst A: General, 318,2007, 108-120.

[14]. D. K. Chattopadhyay, K. M. Aswini, B. Sreedhar,K.V.S.N. Raju, Thermal and viscoelastic properties of polyurethane-imide/clay hybrid coatings, Polymer Degradation and Stability, 91, 2006,1837-1849.
[15]. L. Petersson, K. Oksman, Biopolymer based nanocomposites: Comparing layered silicates and microcrystalline cellulose as nano-reinforcement, Composite Science and Technology, 66(13),2006, 2187-2196.
[16]. H. D. Cheol, H. L. Min, D. K. Young, H. M. Byong, H. K. Jeong, Effect of clay modifiers on the morphology and physical properties of thermoplastic polyurethane/clay nanocomposites, Polymer, 47,2006, 6718- 6730
[17]. H. Zheng, Y. Zhang, Z. Peng, Influence of clay modification on the structure and mechanical properties of EPDM/montmorillonite nanocomposites, Polymer Testing, 23(2),2004, 217-223
[18]. Y. W. Chen-Yang, H. C. Yang, G. J. Li,Y. K. Li, Thermal and anticorrosive properties of polyurethane/clay nanocomposites, Journal of Polymer Research,11(4), 2005,275-283.
[19]. Y.W. Chen-Yang, Y.K. Lee, Y.T. Chen, J.C. Wu,High improvement in the properties of exfoliated PU/clay nanocomposites by the alternative swelling process, Polymer,48,2007, 2969-2979
[20]. C. Feina, C. J. Sadhan, Nanoclay tethered shape memory polyurethane nanocomposites, Polymer, 48,2007, 3790-3800.
[21]. A. Leszczy´nska, J. Njuguna, K. Pielichowski, J.R. Banerjee, Polymer/montmorillonite nanocomposites with improved thermal properties: Part I. Factors influencing thermal stability and mechanisms of thermal stability improvement, Thermochimica Acta, 454, 2007, 75-96
[22]. S. Sankaraiah, C. Sung-Wook, L. Jun-Young, K. Jung-Hyun, Aqueous dispersion of novel silylated (polyurethane-acrylic hybrid/clay) nanocomposite,Polymer, 48(16), 2007, 4691-4703.
[23]. G. R. F. Florêncio,J. A. M. Tomás, S. R. Marcelo, M. L. S. Suédina, Thermal stability of nanocomposites based on polypropylene and bentonite, Polymer Degradation& Stability, 89(3),2005, 383-392.
[24]. Gilman, J W. Flammability and thermal stability studies of polymer layered-silicates (clay) nanocomposites,Applied Clay Science, 15,1999, 31-49.
[25]. S. Austin, C. H. Patrice, C. Valeska, D. S. Ronald, Use of acrylic based surfmers for the preparation of exfoliated Polystyrene-clay nanocomposites, Polymer, 48,2007, 1490-1499
[26]. J.E. Bradby, J.S. Williams, M.V. Swain, Pop-in events induced by spherical indentation in compound semiconductors, Journal Material Research, 19 (1) 2004, 380–386.
[27]. Oliver, W. C.; Pharr, G. M. Measurement of hardness and elastic modulus by instrumented indentation: Advances in understanding and refinements to methodology, Journal of Material Research, 19 (1)2004, 3-20.
[28]. Y. Hua, L. Shen, H. Yang, M. Wang, T. Liud, T. Lianga,J. Zhanga, Nanoindentation studies on Nylon 11/clay nanocomposites,Polymer Testing, 25(4),2006, 492–497
[29]. L. Shen, I. Y. Phang, L. Tianxi,Nanoindentation studies on polymorphism of nylon 6, Polymer Testing, 25,2006, 249-253
[30]. G. E. Kraus, Reinforcement of Elastomers(Wiley, New York, 1965).
[31]. M. Alexandre, P. Dubois, Polymer-layered silicate nanocomposites: preparation, properties and uses of a new class of materials, Material Science Engeneering, 28 (24)2000, 1-63.
[32]. A. Himadri, S. K. Suneel, Influence of nanodispersed organoclay on rheological and swelling properties of ethylene propylene diene terpolymer, Macromolecular Research, 14 (2),2006, 132-139
[33]. S. Ranimol, C. Ranganathaiah, V. Siby, J. Kuruvilla, T. Sabu, Gas transport through nano and micro composites of natural rubber (NR) and their blends with carboxylated styrene butadiene rubber (XSBR) latex membranes, Polymer,47(3),2006,858-870.
[34]. A. M. Motawie, M.Madani, E.A.Esmail, A.Z.Dacrorry, H.M. Othman, M.M.Badr,D.E. Abulyazied, Electrophysical characteristics of polyurethane/organo-bentonite nanocomposites, Egyptian Journal ofPetroleum, 23 (4)2014,In Press.
[35]. H.Zheng, Y. Zhang,Z.Peng, Y.Zhang, Influence of clay modification on the structure and mechanical properties of EPDM/montmorillonite nanocomposites, Polymer Testing,23(2),2004, 217-223.
[36]. M. Madani, Effect of Irradiation on theProperties of Rubber- Based Conductive BlendComposites, Polymer& Polymer Composites, 17,2004, 525-534.
[37]. M. Madani and A.I. Abd-El Hafez, X-ray Shielding Ability and Electrophysical Characteristics of Rubber Vulcanizates: Effect of State-of-Mix, Particle PhysicsInsights, 3,2010, 9-22.
[38]. N.S. Karybiants, O.E. Philippova, S.G. Starodubtsev, A.R. Khokhlov, Conformational transitions in poly(methacrylic acid) gel/poly(ethylene glycol) complexes. Effect of the gel cross-linking density,Macromolecular Chemistry and Physics, 197,1996, 2373.
[39]. P.J. Flory, J. Rehner, Statistical Mechanics of Cross-Linked Polymer Networks II. Swelling, Journalof Chemical Physics, 11,1943,521-526.
[40]. LE. Nielsen, Cross-Linking-Effect on Physical Properties of Polymers, Journal of Macromolecular Science, Part C - Reviews in Macromolecular Chemistry,C3,1969, 69-103.
[41]. P. Wenyi, H. Xingyi, Y. Jinhong, J. Pingkai, L. Wenhao, Electrical and thermo-physical properties of epoxy/aluminum nitride nanocomposites: Effects of nanoparticle surface modification Composites: Part A, 41,2010, 1201–1209.
[42]. M. Y. Abed, D. Elsawy, N. A. Mansour, M. G. Mohamed, A. Ashary, A. Mazrouaa, Synthesis and Investigation of Pillared Layered/ Pyrrole, Material Science an Indian Journal, 10 ,2014, 205-212.
[43]. Y. Chun-Chen, Study of alkaline nanocomposite polymer electrolytes based on PVA–ZrO2–KOH, Material Science and Engineering B,131, 2006, 256-262.